Research Paper

Thermal effect of percutaneous radiofrequency ablation with a clustered electrode for vertebral tumors: In vitro and vivo experiments and clinical application

Zhao Wei, Peng Zhao-Hong, Chen Jin-Zhou, Hu Ji-Hong, Huang Jian-Qiang, Jiang Yong-Neng, Luo Gang, Yi Gen-Fa, Wang Hui, Jin Shen, Gao Bu-Lang*

Department of Medical Imaging, The First Affiliated Hospital, Kunming Medical University, 295 Xichang Road, Kunming 650032, Yunnan, PR China

ABSTRACT

Purpose: To investigate effects and heat distribution of radiofrequency ablation (RFA) on vertebral tumors in vitro and in vivo swine experiments and its clinical application.

Materials and methods: RFA was performed on the swine spine in vitro and in vivo for 20 min at 90 °C at the electrode tip, and the temperature at the electrode tip and surrounding tissues were recorded. Clinical application of ablation combined with vertebroplasty was subsequently performed in 4 patients with spinal tumors.

Results: In the in vitro study, the mean temperature at the front and ventral wall of the spinal canal was 50.8 °C and 43.6 °C, respectively, at 20 mm significantly greater than 37.7 °C and 33.7 $\pm$ 1.7 °C, respectively, at 10 mm ablation depth. The coagulative necrosis area was significantly ($P < 0.0001$) greater at 20 mm depth than at 10 mm depth (mean 17.0×20.7 mm^2 vs. 14.2×16.6 mm^2). In the in vivo experiment, the local temperature increased significantly ($P < 0.05$) from around 36 °C before ablation to over 41 °C at 20 min after ablation, with the temperature at the electrode tip (90.4 °C) and within the vertebral body (67.0 °C) significantly ($P < 0.05$) greater than at the posterior (41.9 °C) and lateral wall (41.8 °C). From 2 to 5 weeks, bone remodeling began. Clinically, all four patients had successful RFA and vertebroplasty, with no neurological deficits. The pain scores were significanlty ($P < 0.05$) improved before (4.5–10, mean 8.0) compared with at four weeks (0–1.8, mean 1.8).

Conclusion: The clustered electrode can be efficiently and safely applied in the treatment of spinal tumors without damaging the spinal cord and adjacent nerves by heat distribution.

1. Introduction

Radiofrequency ablation (RFA) was initially developed in the past few decades for treatment of soft tissue tumors and has been proved to be a safe and effective therapeutic option for patients with liver, lung, kidney and bone neoplasms and has been increasingly performed in clinical settings [1–10]. Ever since the first application of RFA in the bone tissue for treating osteoid osteoma was reported in 1992 [11], this technique has been employed for more bone tumors including chondroblastoma [12], chondromas [13], and osteolytic metastasis [14]. However, when tumors are adjacent to nerves, risk of nerve injury may exist in RFA, especially because the current intraprocedural imaging monitoring methods could not clearly detect the gross margin of RFA necrosis. This limits the application of RFA. Neural damage by RFA is one of the most serious complications of the ablation procedure and has

been recorded in patients with spinal tumors adjacent to nerves [15–17]. RFA produces ionic oscillation and subsequent friction heat to destroy tissues through thermal coagulative necrosis, and the heat delivered to the tumor tissue is responsible for neural injury. The temperature in the tumor may reach 100 °C during RFA, and this heat may be transferred to adjacent nerves. Nerve injury takes place when the spinal canal temperature achieves 45 °C, and it is considered unsuitable for RFA if the spinal tumors were located within 1 cm to the spinal cord [18]. The major concern with thermal ablation for spinal tumors is injury to the spinal cord and nerves if ablation is applied adjacent to the posterior vertebral body wall or in epidural tissues. Moreover, in bone and in the spine in particular, RFA is more difficult than in soft tissues due to unpredictable bone environment surrounding the targeted lesion. Even though some RFA studies have been carried out for patients with primary or metastatic spinal tumors [19–22], no detailed animal
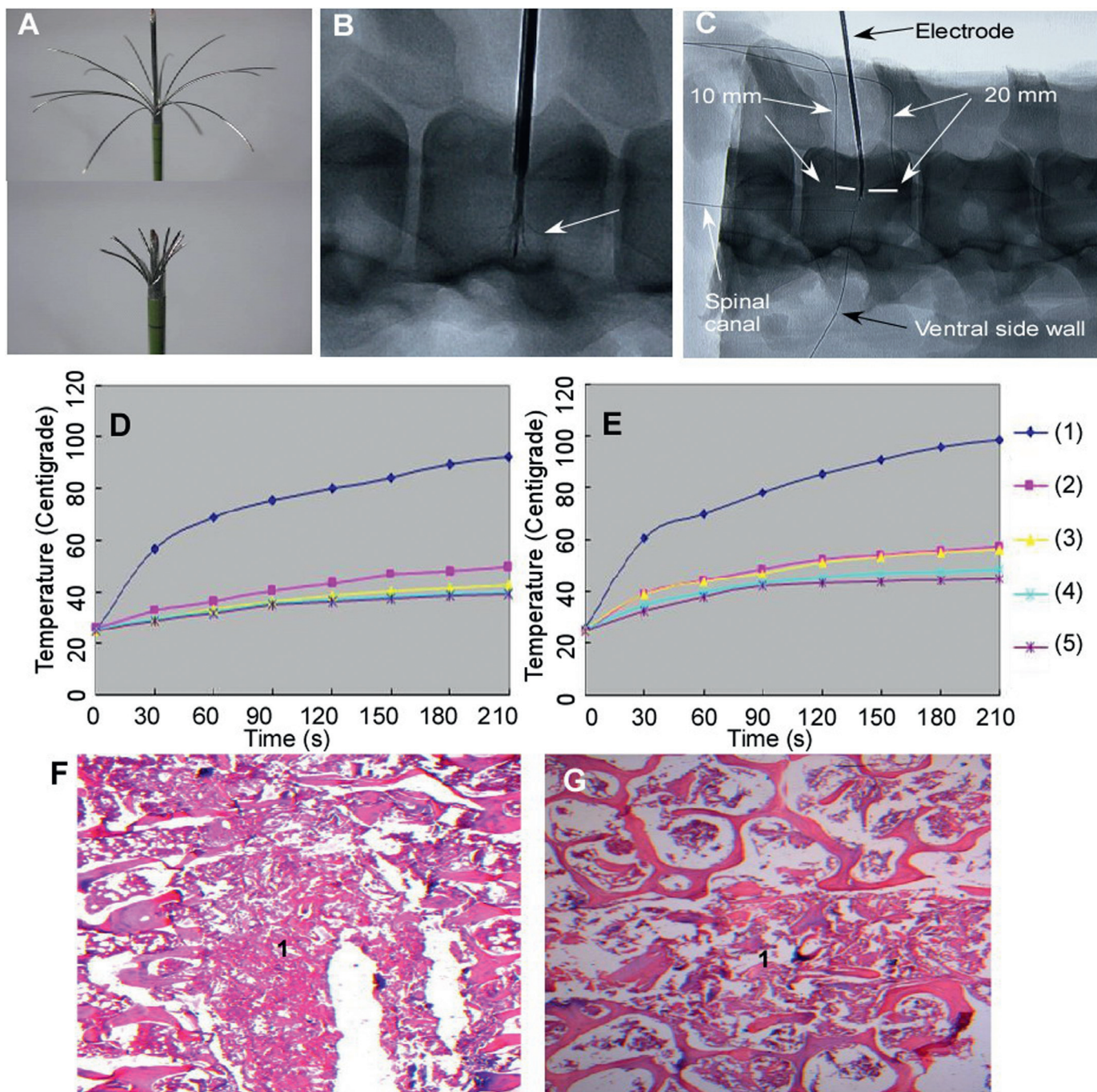
Fig. 1. In vitro study. (A) The hooked array electrode for radiofrequency ablation has 13 hooks. (B) The electrode was sent into a vertebral body with the array electrode partially opened (arrow). (C) The distribution of ablation and temperature sensors. Two temperature sensors were located 10 and 20 mm away from the electrode needle, respectively, the third (indicated by spinal canal) on the front wall of the spinal canal, and the last one on the ventral side wall of the vertebral body. 10 mm indicates the temperature senor is located 10 mm from the electrode tip while 20 mm the senor 20 mm from the electrod tip. Ventral side wall indicates the sensor is on the ventral side of the vertebral body while spinal canal indicates the sensor is on the spinal canal front wall or the posteiror wall of the vertebral body. (C, D) Temperature changes were detected during the initial 210 s when the electrode needle was inserted 10 mm (C) and 20 mm (D) inside the vertebral body. Line 1 indicates a temperature sensor at the center of electrode, line 2 indicates a sensor at 10 mm away from the eletrode tip within the vertebral body, line 3 indicates a sensor at the front wall of the spinal canal, line 4 indicates a sensor at the ventral side wall of the vertebral body, and line 5 indicates a sensor at 20 mm away from the elctrode within the vertebral body. (E, F). Histopathology revealed coagulation necrosis (1) of the bone trabecula structure with no osteocytes at the center of the electrode (E) and 1.5 cm away from the electrode tip (F). The trabecula was destroyed much more in the center than 1.5 cm away.

experiments have been performed to investigate heat distribution in targeted spinal lesions and surrounding tissues of spinal cord and nerves especially in RFA with a clustered electrode. We hypothesized that because of lack of animal experiments investigating heat distribution in the spinal canal and surrounding tissues in RFA for spinal tumors, no generally accepted protocols for RFA in spinal tumors exist especially regarding a clustered electrode for RFA. This study was consequently designed to investigate the effect of RFA and heat distribution in spinal canal and around the vertebral bodies in swine experiments in vitro and vivo, and based on these experiments, we subsequently treated some patients with spinal tumors.

2. Materials and methods

2.1. RFA generator

The RFA equipment used was a commercial RFA generator RFA-I (Beijing Bolai, Beijing, China) which is capable of producing a maximal output of 300 W., 330 kHz and 110 °C. The electrode needle for this RFA generator has 13 hooked electrodes (Fig. 1, RFA-1315, Beijing Bolai, Beijing, China). The cluster needle has a diameter of 3.9 cm at complete opening, and one single albation can create a necrosis area of 5–6 cm diameter. Ablation can also be performed with the cluster needle half opened to produce smaller ablation areas, but the necrosis area is within 2 cm near the tip of each hook. This multi-polar RFA generator can be used for lesions in both soft tissue and bone. When used for bone lesions, both osteolytic and oesteogenic lesions can be ablated with this device. When the front handle of this device is fixed, the multiple electrodes can be pushed forward for release of the hooks or electrodes.

2.2. In vitro studies

The in vitro experiments were performed in air with the air temperature of 20 °C. Thirty vertebral bodies of the swine thoracolumbar spine were obtained from a slaughterhouse and were divided into two groups. A central hole was drilled in the vertebral body for insertion of the RFA electrode needle. Two additional holes were drilled at the same vertebral body at 10 mm and 20 mm to the central hole for placement of remote temperature sensors. Two temperature sensors were also placed at the front wall of the spinal canal and at the ventral side of the vertebral body at the level of the electrode (Fig. 1). RFA was performed with insertion of the ablation electrode tip into the vertebral body for 10 mm (group 1) and 20 mm (group 2) with the electrode tip temperature set at 90 °C and duration of 20 min based on the instruction for use of this device. The temperature was recorded before and after RFA at the four sites.

2.3. In vivo studies

Two fragrant pigs (weighing 52.5 and 57.5 kg) provided by the animal experiment center of our university were used for this study. Approval of the scientific committee on animal research and care was obtained. The pigs were intubated and anesthetized with halothane and placed on the left side on the table (Fig. 2). Cardiac and respiratory parameters were monitored during the whole procedure. Under imaging guidance of the Allura Xper FD-20 flat detectro (Philips Medical System, Best, The Netherlands) with computed tomographic (CT) scanning function, the lumbar vertebral body for ablation was recognized and drilled. The hooked array electrode was sent through the drilled hole into the center of the vertebral body for ablation, with the electrode tip temperature set at 90 °C and duration of ablation at 20 min. The thermistor probes were introduced to 10 mm inside the vertebral body, the posterior and the lateral wall of the vertebral body by a bone puncture needle for recording the temperature at these sites. The temperature was recorded before and at 5, 10, 15 and 20 min of ablation. Pig A had ablation at the fourth and fifth lumbar vertebral bodies and was euthanized immediately following ablation. Pig B was ablated at the third and fifth lumbar vertebral bodies in the first week, at the fourth lumbar and the first sacral vertebral bodies in the second week, at the second lumbar and twelfth thoracic vertebral bodies in the third week, at the first lumbar and eleventh thoracic vertebral bodies in the fourth week, at the eighth and tenth thoracic vertebral bodies in the fifth week, and was euthanized in the sixth week. The ablation was performed in Pig B with an interval of one vertebral body to prevent possible fracture and subsequent paraplegia. Imaging guidance was performed throughout the ablation procedure. After euthanization, the vertebral bodies were sampled and cut into slices of 5 μm with a wet high-speed band saw before fixation in 10% formalin. After decalcification, the bone samples were stained with Hematoxylin–Eosin for histologic examination.

2.4. Clinical studies

Four patients who were diagnosed as vertebral tumors were recruited for this study (Table 3), including 2 males and 2 females with an age range of 54–84 years (mean 68.3). Three patients had vertebral metastasis from lung cancer, lymphoma and primary hepatic carcinoma, respectively, and the remaining one had vertebral angioma. All patients presented with sustained severe pain associated with metastasized malignancy or veretebral angioma. All patients underwent CT, magnetic resonance imaging (MRI) or emission computed tomography (ECT) before RFA for correct diagnosis. All viable treatment approaches, risks and benefits associated with each approach were discussed with the patients. Signed informed consent was obtained from all patients after approval of the hospital ethics committee. After RFA, all patients had radiological, CT or MRI for comparison of the diseased vertebrae and possible cement leakage.

The procedure of RFA and cement injection was performed under the guidance of digital subtraction angiography and fluoroscopic imaging with the patients in the prone position under conscious sedation (Fig. 3). Access to the vertebral body was gained with the Gallini biopsy needle (Mirandola, Italy). RFA was performed with the electrode tip temperature set at 90 °C and duration of 15 min for each location. After completion of the ablation portion of the procedure, the electrode needle was withdrawn, and bone cement (polymethyl methacrylate) was injected into the ablated cavity under fluoscopic guidance. Usually, 3–5 ml bone cement was sufficient to fill the ablated vertebral body cavity. After RFA and bone cement injection, all patients had ragiological check-up to determine distribution of the bone cement. Follow-up was performed 24 and 48 h, one, two and four weeks following the procedure. At follow-up, all patients were asked to rate the level of back pain using an 11-point scale, where 0 stands for no pain and 10 for the worst pain in their lives.

2.5. Statistical analysis

The statistical software SPSS 19 (IBM, Chicago, IL, USA) was used for analysis. Continuous data were expressed as mean ± standard deviation (SD). Student t test was used to compare the difference between two groups, and analysis of variance (ANOVA) was used for comparison among different groups. The significant P was set at < 0.05.

3. Results

3.1. In vitro experiments

Within one minute after initiation of ablation, the temperature went up with increase of the output power of RFA and continued to rise after the power was stabilized. The temperature rose faster and greater near the electrode tip and reached a plateu at 3.5 min (Fig. 1 and Table 1). The temperature was significantly ($P < 0.05$) higher in group 2 compared with group 1, and the mean temperature at the front wall of the spinal canal was 50.8 °C at 20 mm but 37.7 °C at 10 mm ablation depth during the ablation. Histopathological examination showed an elliptical necrosis area with severely damaged structure of the bone. The elliptical necrosis area ranged 12.5–15.3 mm in the short axis and 15.5–17.4 mm in the long axis for group 1 with 10 mm depth ablation but 15.3–18.4 mm in the short axis and 19.1–21.9 mm in the long axis for group 2 with 20 mm depth ablation. The coagulative necrosis area was significantly ($P < 0.0001$) greater in group 2 than in group 1 (mean 17.0×20.7 mm^2 versus 14.2×16.6 mm^2).
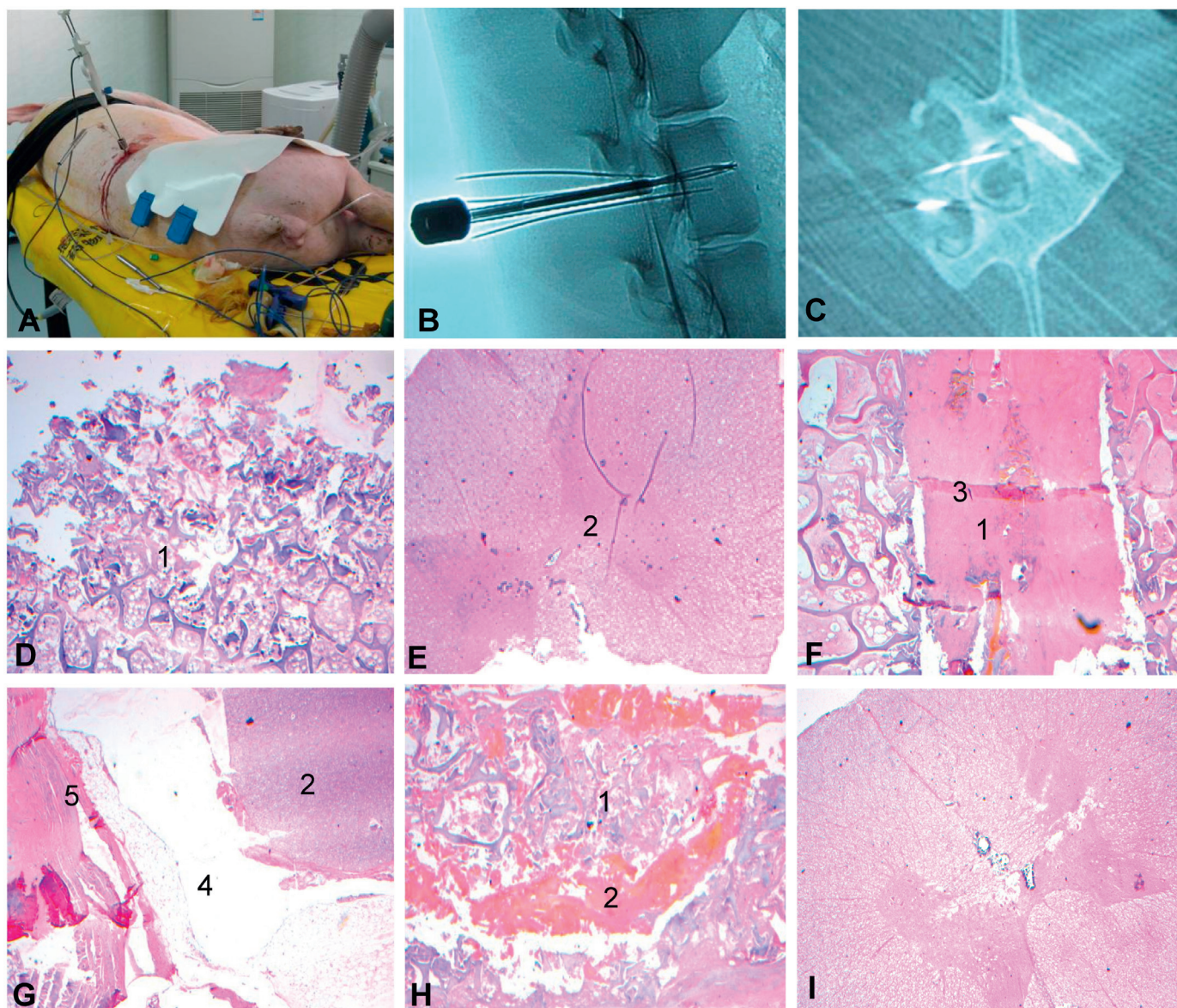
Fig. 2. In vivo study. (A) The pig was laid on the left side for radiofrequency ablation. (B, C) Radiological positioning of the electrode needle and the temperature sensors was demonstrated. Four temperature sensors were located at the electrode tip, 1 cm within the vertebral body, at the posterior and the lateral wall of the vertebral body. (D–I) Histopathology immediately, at 1 and 2 weeks after RFA, respectively, was demonstrated. (D–G) Immediate (D, E) and one-week (F, G) vertebral samples showed coagulative necrosis (D, F) and normal spinal cord structure (E, G). Osteocytes completely disappeared. 1 indicates the bone necrosis with no osteocytes, 2 the normal spinal cord structure, 3 the electrode tract surrounded by bone necroses, 4 the subarachnoid space, and 5 the posterior cortex of vertebral body with some osteocytes. (H–I) Two-week samples revealed the coagulative necrosis (1) surrounded by a band of hemorrhage containing hemosiderin (2). Some granulation tissues began to grow in the band of heorrhage. The spinal cord structure was normal (I).

3.2. In vivo experiments

Both pigs had successful ablation. During the consecutive ablation period, pig B could not stand up on the posterior limbs in the first day post RFA possibly caused by ablation-induced edema to compress the spinal cord, which was resolved by hormone administration on the second day post RFA. No fracture, dislocation, damage to the spinal canal or cerebrospinal fluid leakage occurred during or after the RFA.

The local temperature increased rapidly with rise of the output power in the initial 2.5 min of ablation and reached the plateu at 3 min. The temperature at the electrode center and within the vertebral body went up faster and greater than at the posterior and lateral wall (Fig. 2). Before ablation, the temperature at each site had no significant ($P > 0.05$) difference ranging 36.2 ± 0.22 °C to 36.4 ± 0.36 °C, but five minutes after RFA, a significant ($P < 0.05$) difference was detected

(Table 2). The temperature was significantly ($P < 0.05$) greater and continued to rise more significantly ($P < 0.05$) till the end of ablation at the electrode tip and within the vertebral body than at the posterior and lateral wall.

Immediately after RFA, coagulative necrosis was present in the ablation site (Fig. 2), with severely disordered and destructive trabecula and surrounding band of hemorrhage. Osteocytes were all destroyed. Neighboring vertebral bodies remain intact. One week later, the vertebral sample demonstrated coagulative necrosis and hemorrhage with intact vertebral bodies and spinal cord. No osteocytes were present. In two-week samples, the coagulative necrosis was surrounded by a band of hemorrhage containing hemosiderin. Some granulation tissues began to grow in the band of heorrhage, indicating start of repair. The corresponding spinal cord remained intact. In 3-week samples (Fig. 4), a plenty of fibrous tissues grew in the necrosis area indicating apparent
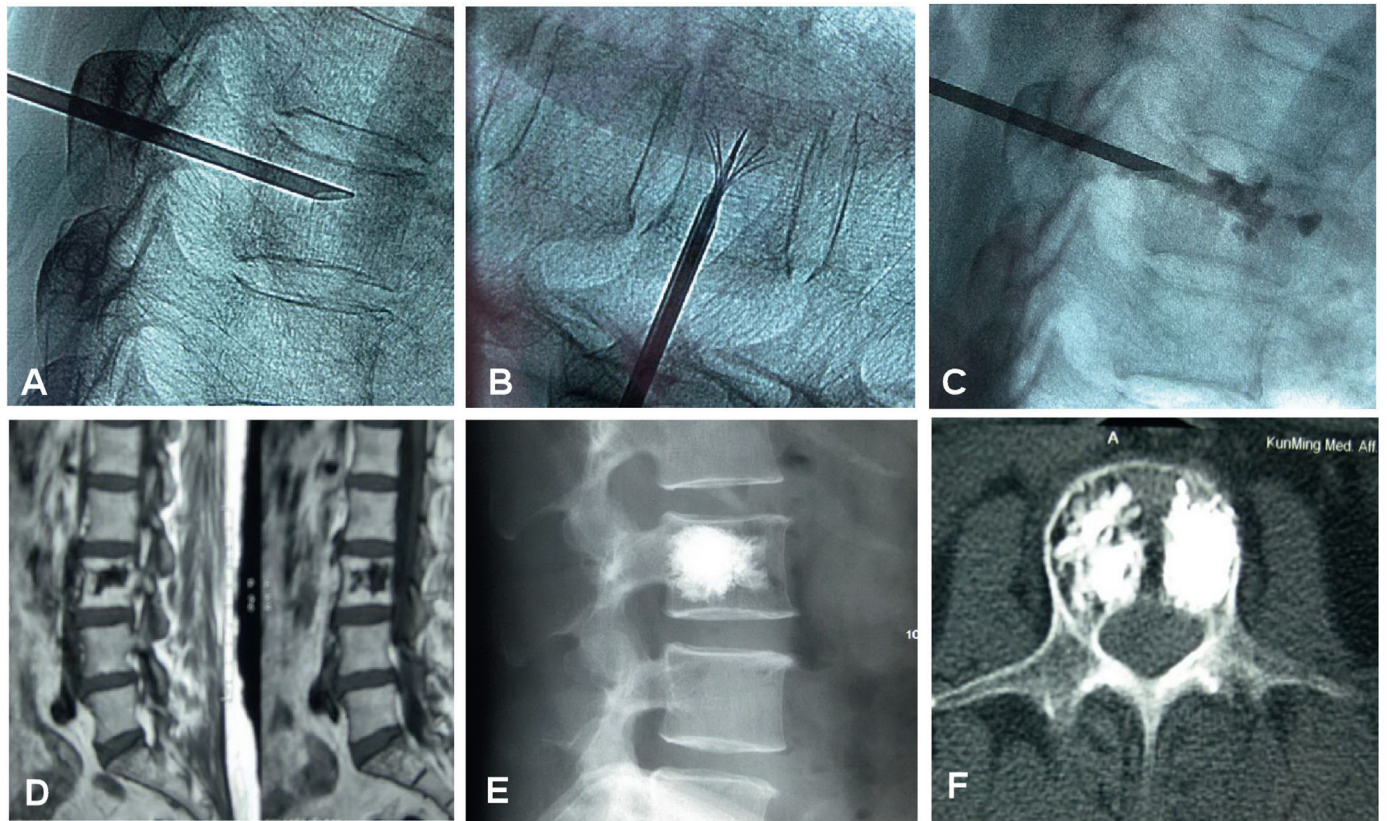
Fig. 3. The combined radiofrequency ablation and percutaneous vertebroplasty with cement injection was performed in patients with spinal tumors. (A) An exterior trocar was inserted into the center of the vertebral body. (B) The clustered electrode with 13 hooks were inserted through the trocar into the vertebral body for ablation. (C) After ablation, the electrode was withdrawn and cement was injected. (D) Magnetic resonance imaging showed an irregular zone of osteolysis in the third lumbar vertebral body. (E, F) After ablation and cement injection, the cement was distributed well in the osteolytic area.

repair. In the forth week, a large quantity of fibrous callus turned to osseous callus, the necrotic area became smaller, and some trabeculas were rebuilt to the normal structure. In 5-week samples, the osseous callus continued to increase and was rebuilt into complete normal trabecula, and the RFA-induced coagulative necrosis area continued to shrink. During the five week period, the neighboring vertebral bodies and the spinal cord remained intact with no injury or destruction.

3.3. Clinical application

All patients had successful RFA and bone cement injection. In one patient who had metastatic destruction of the vertebral body posterior wall, the bone cement leaked and compressed one lateral nerve root, causing local pain. No other complications occurred. The leaked cement was surgically removed two days later and the pain was remarkably improved. Before the procedure, the pain level ranged 4.5–10 scores (mean 8.0). After the procedure, the pain scores were 2.1–7.8 (mean 5.9) at 24 h, 1.9–7.5 (mean 5.2) at 48 h, 1.0–3.1 (mean 2.6) at one week, 0–2.0 (mean 2.0) at two week, and 0–1.8 (mean 1.8) at four week (Fig. 5). The pain was significantly ($P < 0.01$) improved after the procedure, especially at one week.

Table 2

In vivo temperature (°C) at different probing sites during ablation.

Time (min)	Electrode center	1 cm within	Posterior wall	Lateral wall	P
0	36.4 ± 0.36	36.2 ± 0.22	36.2 ± 0.34	36.3 ± 0.18	0.38
5	90.1 ± 0.09	63.5 ± 3.31	41.3 ± 0.83	41.6 ± 0.94	0.00
10	90.2 ± 0.23	65.9 ± 2.32	41.6 ± 0.92	41.5 ± 0.58	0.00
15	90.3 ± 0.17	66.8 ± 1.83	41.8 ± 0.71	41.7 ± 0.49	0.00
20	90.4 ± 0.24	67.0 ± 1.26	41.9 ± 0.86	41.8 ± 0.61	0.00
P*	0.02	0.00	0.24	0.89	

Note: *P indicates comparison from 5 min to 20 min excluding time 0. Posterior wall indicates the posterior wall of the vertebral body while the lateral wall indicates the lateral wall or surface of the vertebral body.

Radiological examination revealed good filling of bone cement in all the osteolytic area except for one patient who had cement leakage (Fig. 3). The vertebral bodies remained intact in the rest three patients.

4. Discussion

In this study, we first investigated the effect of RFA and heat

Table 1

In vitro temperature (°C) at all sites from 3.5 min till the end of ablation (20 min).

Ablation depth (mm)	Electrode tip	20 mm away	10 mm away	Front wall	Ventral wall
Group 1 (10)	92.6 ± 2.8	35.3 ± 2.6	45.9 ± 2.5	37.7 ± 2.0	33.7 ± 1.7
Group 2 (20)	93.7 ± 4.1	40.0 ± 2.5	51.5 ± 2.9	50.8 ± 2.5	43.6 ± 2.4

Note: 10 and 20 mm away means from the electrode tip, front wall indicates the front wall of the spinal canal, and ventral wall the ventral wall of the vertebral body. Significant difference ($P < 0.0001$) existed in the temperature between 10 mm and 20 mm sites.

Table 3
Demographic data.

No./sex/age	History	Tumor location	Type
1/F/84	Lung cancer for 3 m	4th and 5th thoracic vertebra metastasis	Osteolytic
2/F/56	Vertebral angioma for 12 m	3rd lumbar and alae sacralis	Osteolytic
3/M/79	Lymphoma for 4 m	6th thoracic vertebra metastasis	Osteolytic
4/M/54	Primary hepatic cancer for 3 m	4th lumbar metastasis	Osteolytic

Note: F, female; M, male; m, months.

distribution in the spinal canal and subsequently successfully treated some spinal tumors using combination of RFA and cement injection for vertebral augmentation, achieving some good results. The clinical application of RFA in combination with cement injection can be safely performed in the vertebral bodies, resulting in improved quality of life with no cytotoxic thermal effect on the spinal cord. In the in vitro experiment in our study, the temperature of the front wall and ventral wall of the spinal canal was 50.8 ± 2.5 °C and 43.6 ± 2.4 °C, respectively, when the temperature sensor was 20 mm away from the electrode tip but 37.7 ± 2.0 °C and 33.7 ± 1.7 °C, respectively, when the temperature sensor was 10 mm away from the electrode tip. This indicates that the position of the electrode tip affects the temperature in the spinal canal, and we should control the position of the electrode tip so that excessive temperature cannot be produce in the spinal canal to damage the spinal cord or nerves. In the in vivo experiments in the porcine, the temperature at the posterior wall of vertebral body was the maximal of 43.3 °C with the mean value of 41 °C which did not exceed the limit of 45 °C to damage the spinal cord [29,30]. Since the in vivo

vertebral body has rich epidural venous plexus and the spinal canal has rich cerebrospinal fluid, the actual temperature can be decreased by local heat sinks caused by this blood and fluid flow. Moreover, good control and positioning of the electrode tip can also be used to control the heat distribution on the wall of the spinal canal for prevention of damage to the spinal cord and surrounding nerves.

A monopolar electrode may produce a coagulative necrosis area ≦1.6 cm in diameter, whereas an internally cooled radiofrequency electrode may create larger regions of coagulative necrosis approaching 5 cm with a single electrode [23] but 7 cm with a cluster of three electrodes [24] in soft tissues. The earliest RFAs were performed with monopolar electrodes which could only create the maximal coagulation diameter of 1.6 cm and were not adequate for most tumors. However, as modification of RFA electrode design has advanced with development of multiprobe arrays, bipolar arrays, internally cooled electrodes and cluster or pulsed radiofrequency, a significantly increased coagulation area can now be achieved [25]. After studying radiofrequency ablation in pig spine with an internally cooled electrode containing an adjustable tip, You et al. [25] found that the coagulation area was 4.19 ± 2.95 cm^3 (1.26–3.05 cm in diameter) in an in vitro experiment but 6.80 ± 2.72 cm^3 (1.28–2.51 cm in diameter) in an in vivo experiment, with the average temperature in the epidural space of the pig of 34.9 °C at the end of 20-min ablation but 38.2 °C at the end of 30-min ablation. After evaluation of a bipolar-cooled RFA device for bone metastases in porcine vertebrae, Pezeshki et al. [26] found that the coagulation necrosis volume created by this bipolar device was 2.24 ± 0.90 cm^3 with the mean temperature on the surface of the vertebral body of 36.1 °C (range 32–40 °C) at the end of 15-min ablation. Tillotson et al. [27] reported an area of coagulative necrosis of 9–13 mm using a monopolar electrode for RFA in a bone tumor model regardless of the probe size or duration of heating. Currently, no studies have been performed with a clustered electrode of 13 hooks in
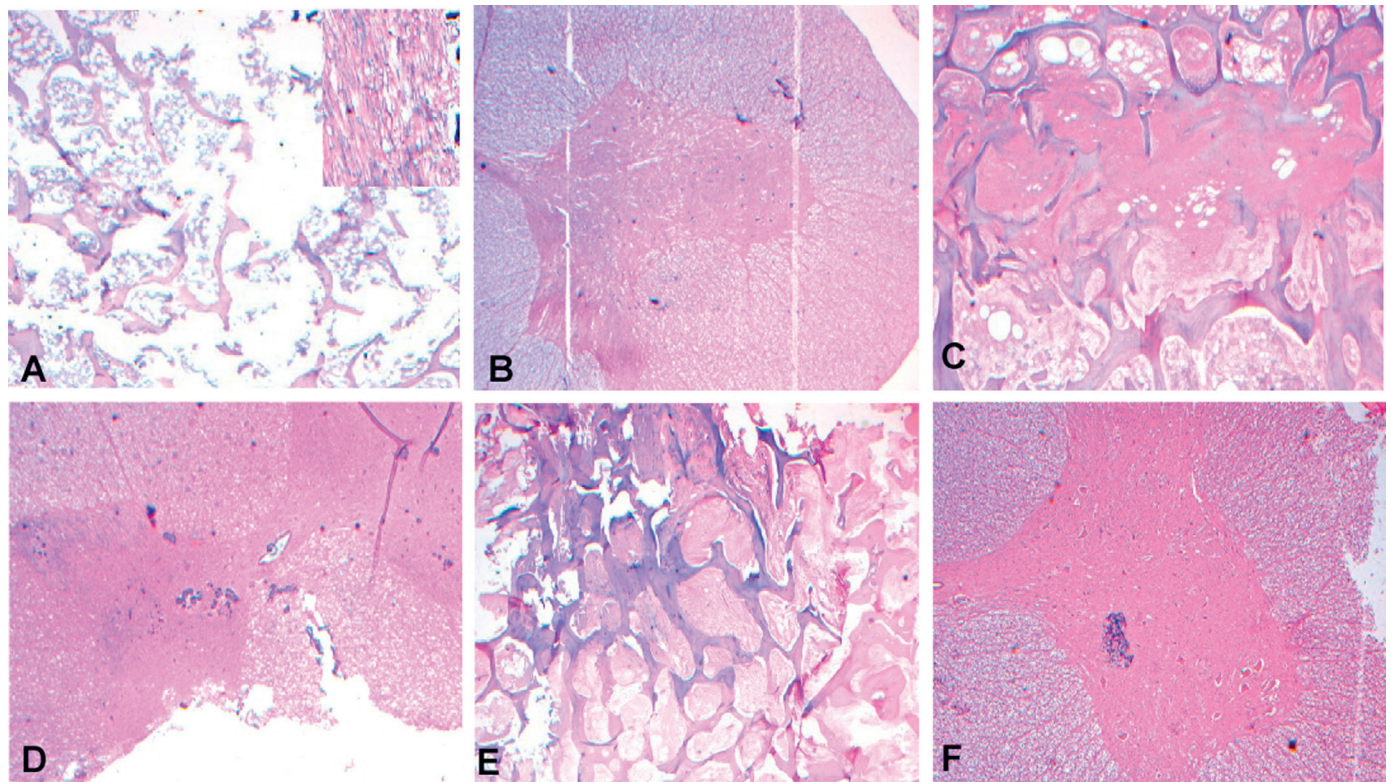

Fig. 4. (A–F) Histopathology at 3–5 weeks after RFA, respectively, was demonstrated. (A, B) In 3-week samples, a plenty of fibrous tissues (inserted figure in A) grew in the necrosis area (A), and the spinal cord structure was normal (B). (C, D) In the forth week, a large quantity of fibrous callus turned to osseous callus, and some trabeculas were rebuilt into normal structure (C) with noramal structure of the spinal cord (D). (E, F) In 5-week samples, the osseous callus continued to proliferate and was rebuilt into complete normal trabecula (E). The spinal cord was normal (F).
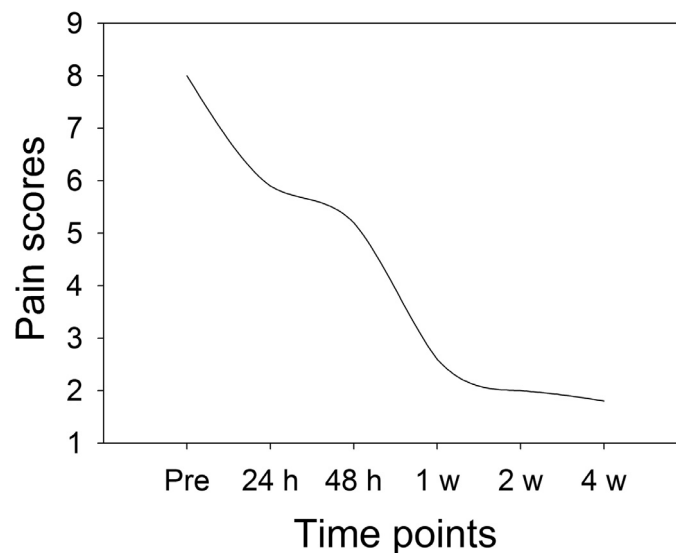
Fig. 5. Pain scores were significantly ($P < 0.005$) decreased at each time point after compared with before ablation.

animals and investigated the repair process of bone after RFA created coagulation necrosis in the spine like ours. In our study, we used a cluster of 13 electrodes which have a diameter of 3.9 cm when fully opend, and one single ablation can produce a necrosis area of 5–6 cm diameter in soft tissue, much larger than that created by an internally cooled or bipolar electrode. Ablation can also be performed with the cluster needle half opened creating smaller ablation areas within 2 cm arround the tip of each hook. For monopolar or bipolar electrodes, the area of coagulation necrosis of ablation cannot be increased or adjusted, whereas the area of coagulation necrosis creaed by our multi-polar electrodes can be adjusted through regulating the size of opening of the electrode hooks. In our in vitro study, the clustered electrode produced a mean coagulative necrosis area of 14.2 mm $\times$ 16.6 mm when inserted 10 mm but 17.0 mm $\times$ 20.7 mm when inserted 20 mm into the vertebral body, and this may be caused by exposure of more part of the electrode hooks into the vertebral body. The temperature on the posterior wall surface of the vertebral body in the in vivo experiments in the porcine was the maximal of 43.3 °C with the mean value of 41 °C, comparable to those of other studies. RFA has been used mostly for lesions in the lower extremities but less frequently for vertebral lesions due to possible injury to the neural tissue. In a study with a single internally cooled radiofrequency electrode, Dupuy et al. [28] found that the cancellus and cortical bone had some insulating effect to prevent heat transmission and that the temperature in the epidural space was 44 °C when the electrode tip was 10 mm inside the vertebral body. Froese et al. [29] investigated the sensitivity of the thoracolumbar spinal cord of mouse to radiofrequency hyperthermia and found that the spinal cord was damaged when the temperature was 45 °C lasting for 10.8 min. Becasue the radiofrequency heating at about 45 °C has been shown to damage the spinal cord [29,30] and peripheral nerves [31], the radiofrequency effect on the spinal cord and adjacent nerves must be considered when applying RFA in spinal tumors. In our in vitro study, the maximal temperature was only 42.5 °C at the front wall of the spinal canal and 42 °C at the ventral wall of the vertebral body when the electrode tip was 10 mm inside the vertebral body. These temperature values are safe for the spinal cord, adjacent nerves and the abdominal aorta in front of the vertebral bodies. Even if the maximal temperature was 56.3 °C (mean 50.8) at the spinal canal front wall in the in vitro experiment surpassing the 45 °C limit, it was only 43.3 °C in the in vivo pig experiment and remained relatively stable throughout the procedure, with no cytotoxocity to the spinal cord and adjacent nerves. The temperature difference between in vitro and in vivo experiments may be caused by local heat sinks from the rich epidural venous plexus and cerebrospinal fluid pulsations in vivo [28]. This cooling effect of the tissue mediated by blood flow has been shown to negatively influence the scope of coagulation which can be created in vivo hepatic tissue, whereas decrease in blood flow by mechanical or pharmacologic means can increase the area of coagulative necrosis [32]. Moreover, one pig had RFA for five times in 10 vertebral bodies without causing paralysis (no damage to the spinal cord or nerves) in our study. This pig could not stand up on the posterior limbs in the first day post RFA possibly caused by ablation-induced edema to compress the spinal cord, which was resolved by hormone administration on the second day post RFA. This indicates that no injury could be induced to the spinal cord or nearby nerves if the electrode tip, either of one single hook or a cluster of hooks, was controlled at the center of the vertebral body.

Our study demonstrated the changes of the vertebral body from the initial coagulation necrosis caused by RFA to gradual repair in the fifth week. Immediately after RFA, the ablated area had coagulative necrosis with collapsed bone trabecula and disappearance of normal bone structure accompanied with hemorrhage surrounding the necrosis. In the first week following RFA, no apparent repair appeared in the ablated area. From the second week on, organization of the hematoma was started, which was followed by formation of granulation, fibrous tissue and callus. In the fifth week, the fibrous callus turned to osseous callus, some of which was rebuilt into normal bone trabecula. The repair and healing process was like that of bone fracture. In using a bi-polar-cooled RFA device for ablation of bone metastases in porcine vertebral body, Pezeshiki et al. [26] demonstrated that the immediate coagulative necrosis area after RFA was mostly replaced by fibrous tissue, inflammatory cells, new vessels and live osteocytes and osteoblasts in 14-day samples. After studying the in vivo effects of RFA and the repair process in swine long bones using a clustered electrode, Zhao et al. [33] found that the iniital coagualtion necrosis area was an elliptic pale zone surrounded by a narrow brown hemorrhagic band and was replaced by proliferated granulation, fibrous tissue and fresh and mature bone trabecula from day 10 until week 12 after ablation. Yamamoto et al. [34] also reported bone remodeling and proliferation of osteoblasts 30 days after RFA in normal rabbit bone.

Spinal metastasis affects $5-10\%$ of patients with cancer, and about 90% of symptomatic patients suffer from severe pain due to biochemical stimulation, tumor mass effect and related pathologic fracture [26,35–41]. These patients are also at high risk of metastatic spinal cord compression caused by tumor extension and pathological fracture of vertebral bodies, resulting in decreased quality of life and shortened life expectancy [42]. Combined RFA and vertebral cement injection is

an emerging therapy for patients with spinal metastasis [3,4,28]. Percutaneous cement injection (vertebroplasty) is widely used to treat vertebral compression fracture resulted from hemangioma and osteolytic metastases [4,43]. In our study, the RFA was used to necrotize the spinal metastases and hemangioma, whereas the injected cement could prevent the vertebral bodies from fracture. The combination of RFA and vertebroplasty can be safely performed if the posterior vertebral body cortex is intact [17]. Nakatsuka et al. [17] reported severe damage in 4 of 15 patients with spinal tumors which had invaded the posterior cortex of the vertebral body or pedicle. In our study, cement leakage occurred in one patient with metastatic destruction of the posterior vertebral body cortex, the bone cement leaked and compressed one lateral nerve root.

Vertebral hemangiomas are benign and involve the spine with an incidence of 10–12% usually found in young people, predominantly females [44–47]. Most vertebral hemangiomas are asymptomatic incidentally found during imaging examination [46,47]. However, some are aggressive, symptomatic hemangiomas with extraosseous extension or significant osseous expansion due to pathologic fracture, osseous expansion and/or extraosseous extension, leading to mass effect on adjacent neural structures (spinal cord and nerve roots) and accounts for approximately 1% of spinal haemangiomas [44,45]. No studies have investigated spinal hemangioma treated with RFA followed by bone cement injection in the literature. Kaoudi et al. [48] reported robot-assisted RFA of a sacral S1–S2 aggressive hemangioma in a 57-year-old patient, resulting in a satisfying outcome including decreased pain intensity, discontinuation of analgesics, resumation of daily activities, and substantial regression of tumor volume without invation of the vertebral canal on magnetic resonance imaging. In our study, the vertebral hemangioma was in a 54-year-old man which was treated with RFA followed by bone cement injection to strengthen the osteolytic vertebral body, good outcomes were achieved for this patient at follow-up with no pain.

This study has some limitations. Firstly, the in vivo swine experiment did not have longer follow-up time, and longer periods of follow-up in more swines may be needed to reveal the bone modeling process. Secondly, we did not use thermodetectors to monitor the real temperature in the spinal canal when treating patients with spinal tumors. Moreover, the case series was too small, and more patients are needed in the future to prospectively investigate the effect of RFA in a randomized way and multiple centers.

In conclusion, the clustered electrode can be efficiently and safely applied in the treatment of spinal tumors without damaging the spinal cord and adjacent nerves by heat distribution.

Funding

No funding for this work.

Conflict of interest

The authors declared that they have no conflict of interest in publication of this article.

Ethical approval

All applicable international, national, and/or institutional guidelines for the care and use of animals were followed.

All procedures performed in studies involving human participants were in accordance with the ethical standards of the institutional and/or national research committee and with the 1964 Helsinki declaration and its later amendments or comparable ethical standards.

Informed consent

Informed consent was obtained from all individual participants included in the study.

Ethical statement

This study was approved by the ethic committee of The First Affiliated Hospital, Kunming Medical University for scientific research with signed informed consent provided by all participants.

Supplementary materials

Supplementary material associated with this article can be found, in the online version, at doi:10.1016/j.jbo.2018.07.001.

References

[1] R.R. Corby, G.S. Stacy, T.D. Peabody, L.B. Dixon, Radiofrequency ablation of solitary eosinophilic granuloma of bone, Am. J. Roentgenol. (AJR) 190 (2008) 1492–1494.
[2] D.K. Filippiadis, S. Tutton, A. Mazioti, A. Kelekis, Percutaneous image-guided ablation of bone and soft tissue tumours: a review of available techniques and protective measures, Insights Imaging 5 (2014) 339–346.
[3] B.A. Georgy, Bone cement deposition patterns with plasma-mediated radio-frequency ablation and cement augmentation for advanced metastatic spine lesions, Am. J. Neuroradiol. (AJNR) 30 (2009) 1197–1202.
[4] B.A. Georgy, W. Wong, Plasma-mediated radiofrequency ablation assisted percutaneous cement injection for treating advanced malignant vertebral compression fractures, Am. J. Neuroradiol. (AJNR) 28 (2007) 700–705.
[5] Health Quality Ontario, Ont. Health Technol. Assess. Ser. 16 (2016) 1–202.
[6] R.E. Jacobson, M. Granville, D.J. Hatgis, Targeted intraspinal radiofrequency ablation for lumbar spinal stenosis, Cureus 9 (2017) e1090.
[7] X. Liu, Z. Yang, L. Xie, Z. Yuan, M. Ren, L. Han, Advances in the clinical research of the minimally invasive treatment for the posterior edge of vertebral-body defects by spinal metastases, Biomed. Rep. 3 (2015) 621–625.
[8] C. Rossmanna, D. Haemmerich, Review of temperature dependence of thermal properties, dielectric properties, and perfusion of biological tissues at hyperthermic and ablation temperatures, Crit. Rev. Biomed. Eng. 42 (2014) 467–492.
[9] W. Shady, E.N. Petre, M. Gonen, J.P. Erinjeri, K.T. Brown, A.M. Covey, et al., Percutaneous radiofrequency ablation of colorectal cancer liver metastases: factors affecting outcomes – a 10-year experience at a single center, Radiology 278 (2016) 601–611.
[10] P.L. Yang, X.J. He, H.P. Li, Q.J. Zang, G.Y. Wang, Image-guided minimally invasive percutaneous treatment of spinal metastasis, Exp. Ther. Med. 13 (2017) 705–709.
[11] D.I. Rosenthal, A. Alexander, A.E. Rosenberg, D. Springfield, Ablation of osteoid osteomas with a percutaneously placed electrode: a new procedure, Radiology 183 (1992) 29–33.
[12] R.R. Ramnath, D.I. Rosenthal, J. Cates, M. Gebhardt, R.H. Quinn, Intracortical chondroma simulating osteoid osteoma treated by radiofrequency, Skelet. Radiol. 31 (2002) 597–602.
[13] M.R. Callstrom, J.W. Charboneau, M.P. Goetz, J. Rubin, G.Y. Wong, J.A. Sloan, et al., Painful metastases involving bone: feasibility of percutaneous CT- and US-guided radio-frequency ablation, Radiology 224 (2002) 87–97.
[14] F. Rachbauer, J. Mangat, G. Bodner, P. Eichberger, M. Krismer, Heat distribution and heat transport in bone during radiofrequency catheter ablation, Arch. Orthop. Trauma Surg. 123 (2003) 86–90.
[15] M.P. Goetz, M.R. Callstrom, J.W. Charboneau, M.A. Farrell, T.P. Maus, T.J. Welch, et al., Percutaneous image-guided radiofrequency ablation of painful metastases involving bone: a multicenter study, J. Clin. Oncol. 22 (2004) 300–306.
[16] H. Kojima, N. Tanigawa, S. Kariya, A. Komemushi, Y. Shomura, S. Sawada, Clinical assessment of percutaneous radiofrequency ablation for painful metastatic bone tumors, Cardiovasc. Intervent. Radiol. 29 (2006) 1022–1026.
[17] A. Nakatsuka, K. Yamakado, M. Maeda, M. Yasuda, M. Akeboshi, H. Takaki, et al., Radiofrequency ablation combined with bone cement injection for the treatment of bone malignancies, J. Vasc. Interv. Radiol. 15 (2004) 707–712.
[18] A. Nakatsuka, K. Yamakado, H. Takaki, J. Uraki, M. Makita, F. Oshima, et al., Percutaneous radiofrequency ablation of painful spinal tumors adjacent to the spinal cord with real-time monitoring of spinal canal temperature: a prospective study, Cardiovasc. Intervent. Radiol. 32 (2009) 70–75.
[19] T.J. Greenwood, A. Wallace, M.V. Friedman, T.J. Hillen, C.G. Robinson, J.W. Jennings, Combined ablation and radiation therapy of spinal metastases: a novel multimodality treatment approach, Pain Phys. 18 (2015) 573–581.
[20] J.D. Prologo, J. Buethe, K. Mortell, E. Lee, I. Patel, Coblation for metastatic vertebral disease, Diagn. Interv. Radiol. 19 (2013) 508–515.
[21] D. Proschek, A. Kurth, P. Proschek, T.J. Vogl, M.G. Mack, Prospective pilot-study of combined bipolar radiofrequency ablation and application of bone cement in bone metastases, Anticancer Res. 29 (2009) 2787–2792.
[22] E. Rimondi, G. Bianchi, M.C. Malaguti, R. Ciminari, A. Del Baldo, M. Mercuri, et al., Radiofrequency thermoablation of primary non-spinal osteoid osteoma: optimization of the procedure, Eur. Radiol. 15 (2005) 1393–1399.
[23] S.N. Goldberg, G.S. Gazelle, E.F. Halpern, W.J. Rittman, P.R. Mueller, D.I. Rosenthal, Radiofrequency tissue ablation: importance of local temperature along the electrode tip exposure in determining lesion shape and size, Acad. Radiol.

3 (1996) 212–218.

[24] S.N. Goldberg, L. Solbiati, P.F. Hahn, E. Cosman, J.E. Conrad, R. Fogle, et al., Large-volume tissue ablation with radio frequency by using a clustered, internally cooled electrode technique: laboratory and clinical experience in liver metastases, Radiology 209 (1998) 371–379.

[25] N.K. You, H.Y. Lee, D.A. Shin, G.H. Choi, S. Yi, K.N. Kim, D.H. Yoon, J. Park, Radiofrequency ablation of spine: An experimental study in an ex vivo bovine and in vivo swine model for feasibility in spine tumor, Spine 38 (2013) E1121–E1127.

[26] P.S. Pezeshki, J. Woo, M.K. Akens, J.E. Davies, M. Gofeld, C.M. Whyne, et al., Evaluation of a bipolar-cooled radiofrequency device for ablation of bone metastases: preclinical assessment in porcine vertebrae, Spine J. Off. J. N. Am. Spine Soc. 14 (2014) 361–370.

[27] C.L. Tillotson, A.E. Rosenberg, D.I. Rosenthal, Controlled thermal injury of bone. Report of a percutaneous technique using radiofrequency electrode and generator, Investig. Radiol. 24 (1989) 888–892.

[28] D.E. Dupuy, R. Hong, B. Oliver, S.N. Goldberg, Radiofrequency ablation of spinal tumors: temperature distribution in the spinal canal, AJR Am. J. Roentgenol. 175 (2000) 1263–1266.

[29] G. Froese, R.M. Das, P.B. Dunscombe, The sensitivity of the thoracolumbar spinal cord of the mouse to hyperthermia, Radiat. Res. 125 (1991) 173–180.

[30] T. Yamane, A. Tateishi, S. Cho, S. Manabe, M. Yamanashi, A. Dezawa, et al., The effects of hyperthermia on the spinal cord, Spine 17 (1992) 1386–1391.

[31] F.S. Letcher, S. Goldring, The effect of radiofrequency current and heat on peripheral nerve action potential in the cat, J. Neurosurg. 29 (1968) 42–47.

[32] S.N. Goldberg, P.F. Hahn, E.F. Halpern, R.M. Fogle, G.S. Gazelle, Radio-frequency tissue ablation: effect of pharmacologic modulation of blood flow on coagulation diameter, Radiology 209 (1998) 761–767.

[33] W. Zhao, J.Z. Chen, J.H. Hu, J.Q. Huang, Y.N. Jiang, G. Luo, et al., In vivo effects of radiofrequency ablation on long bones and the repair process in swine models, Jpn. J. Radiol. 35 (2017) 31–39.

[34] S. Yamamoto, T. Kaminou, Y. Ono, M. Hashimoto, Y. Ohuchi, H. Yoshida, et al., Thermal influence of radiofrequency ablation for bone: an experimental study in normal rabbit bone, Skelet. Radiol. 43 (2014) 459–465.

[35] S. Bagla, D. Sayed, J. Smirniotopoulos, J. Brower, J. Neal Rutledge, B. Dick, et al., Multicenter prospective clinical series evaluating radiofrequency ablation in the treatment of painful spine metastases, Cardiovasc. Interv. Radiol. 39 (2016) 1289–1297.

[36] L. Capek, P. Henys, P. Barsa, V. Dvorak, Performance of radiofrequency ablation used for metastatic spinal tumor: numerical approach, Proc. Inst. Mech. Eng. Part H J. Eng. Med. 231 (2017) 814–820.

[37] E. David, S. Kaduri, A. Yee, E. Chow, A. Sahgal, S. Chan, et al., Initial single center experience: radiofrequency ablation assisted vertebroplasty and osteoplasty using a bipolar device in the palliation of bone metastases, Ann. Palliat. Med. 6 (2017) 118–124.

[38] N.M. Kam, J. Maingard, H.K. Kok, D. Ranatunga, D. Brooks, W.C. Torreggiani, et al., Combined vertebral augmentation and radiofrequency ablation in the management of spinal metastases: an update, Curr. Treat. Opt. Oncol. 18 (2017) 74.

[39] T.P. Madaelil, A.N. Wallace, J.W. Jennings, Radiofrequency ablation alone or in combination with cementoplasty for local control and pain palliation of sacral metastases: preliminary results in 11 patients, Skelet. Radiol. 45 (2016) 1213–1219.

[40] R. Maugeri, F. Graziano, L. Basile, C. Guli, A. Giugno, G.R. Giammalva, et al., Reconstruction of vertebral body after radiofrequency ablation and augmentation in dorsolumbar metastatic vertebral fracture: analysis of clinical and radiological outcome in a clinical series of 18 patients, Acta Neurochir. Suppl. 124 (2017) 81–86.

[41] W.A. Hall, L.J. Stapleford, C.G. Hadjipanayis, W.J. Curran, I. Crocker, H.K. Shu, Stereotactic body radiosurgery for spinal metastatic disease: an evidence-based review, Int. J. Surg. Oncol. 2011 (2011) 979214.

[42] J.M. Kim, E. Losina, C.M. Bono, A.J. Schoenfeld, J.E. Collins, J.N. Katz, et al., Clinical outcome of metastatic spinal cord compression treated with surgical excision +/- radiation versus radiation therapy alone: a systematic review of literature, Spine 37 (2012) 78–84.

[43] A. Cotten, F. Dewatre, B. Cortet, R. Assaker, D. Leblond, B. Duquesnoy, et al., Percutaneous vertebroplasty for osteolytic metastases and myeloma: effects of the percentage of lesion filling and the leakage of methyl methacrylate at clinical follow-up, Radiology 200 (1996) 525–530.

[44] F.J. Cloran, B.A. Pukenas, L.A. Loevner, C. Aquino, J. Schuster, S. Mohan, Aggressive spinal haemangiomas: imaging correlates to clinical presentation with analysis of treatment algorithm and clinical outcomes, Br. J. Radiol. 88 (2015) 20140771.

[45] M.C. Hurley, B.A. Gross, D. Surdell, A. Shaibani, K. Muro, C.M. Mitchell, et al., Preoperative onyx embolization of aggressive vertebral hemangiomas, Am. J. Neuroradiol. (AJNR) 29 (2008) 1095–1097.

[46] A. Tomasian, A.N. Wallace, J.W. Jennings, Benign spine lesions: advances in techniques for minimally invasive percutaneous treatment, Am. J. Neuroradiol. (AJNR) 38 (2017) 852–861.

[47] J.C. Vilanova, J. Barcelo, J.G. Smirniotopoulos, R. Perez-Andres, M. Villalon, J. Miro, et al., Hemangioma from head to toe: MR imaging with pathologic correlation, RadioGraphics 24 (2004) 367–385 a review publication of the Radiological Society of North America, Inc..

[48] A. Kaoudi, C. Capel, L. Chenin, J. Peltier, M. Lefranc, Robot-assisted radiofrequency ablation of a sacral S1–S2 aggressive hemangioma, World Neurosurg. (2018 May 16), https://doi.org/10.1016/j.wneu.2018.05.060 [Epub ahead of print].